Proc. AIAA Guidance, Naviation and Control Conf., Austin, TX, August 11-14, 2003.

UNFALSIFIED ADAPTIVE SPACECRAFT ATTITUDE CONTROL

Tung-Ching Tsao*[†], Tom Brozenec*, and Michael G. Safonov[‡]

** Boeing Satellite Systems, Inc.*
Los Angeles, California 90009-2919

Abstract

Unfalsified control theory provides a data-driven (model free) formulation of the problems of adaptive and learning control. When applied, it inherently leads to switching. Candidate feedback controllers are switched out of the feedback loop and replaced whenever their ability to meet performance goals is falsified by new experimental evidence. This paper demonstrates how the unfalsified control method can be applied to the problem of antenna mapping control using a simplified spacecraft model. Simulations show that the large uncertainty in spacecraft dynamics falsifies the conventional PID controller design and selects a better one in the controller data bank based only on input/output signals from the plant. This is a truly model free approach to the robust attitude control problem and an innovation in the field of spacecraft attitude control. Potential implementation of this approach is in progress and will be reported in the future.

1. Introduction

The attitude control problem for large, high-powered communication satellites, such as the Boeing Satellite Systems 702 spacecraft illustrated in Figure 1, is characterized by flexible appendages whose modal frequencies are uncertain and whose modal mass, for at least the first few modes, is often significant. It is the presence of this large uncertainty in the spacecraft dynamics which often drives the control design. This is because these flexible appendage modes are characterized by 180 degree phase shifts and typically have significant gain; in addition, the modal frequency uncertainty may be 25% or greater. Robust stabilization (using, for instance, simple roll off gain stabilization filters or, perhaps notch-filter phase stabilization) certainly would not be a problem if modal frequencies were either decades higher than desired attitude control bandwidths or, for notch filter stabilization, simply less uncertain. Unfortunately, this is often not the case. And this is particularly true for the attitude control laws which are used during modes of spacecraft operation which require a relatively fast closed-loop response (note that 0.05 Hz, which in many applications would be considered extremely low, may be considered "high" bandwidth in this context where the first mode frequency may be 0.1 Hz or lower and other physical limitations such as actuator capabilities may limit bandwidth in their linear range). Further complicating matters, these same high bandwidth modes of operation often (though not always) employ chemical propulsion Reaction Control System (RCS) thrusters as the primary means of control actuation, whose inherent "on-off" characteristic will tend to excite flexible modes.

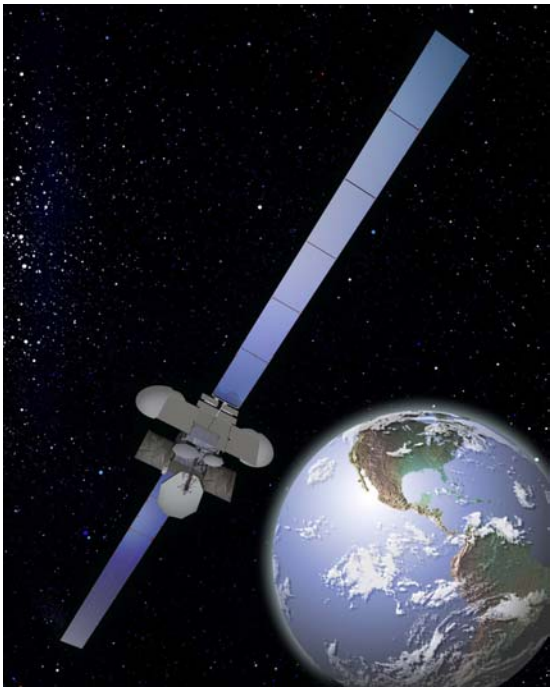

Figure 1 Boeing 702 6-Panel Spacecraft.

One such high bandwidth mode of operation for geosynchronous communication satellites is antenna mapping. This procedure occurs during spacecraft initialization after transfer orbit operations have

[†] Primary contact: Email: tung-ching.tsao@boeing.com, Tel.: 310-416-3025
[‡] Electrical Engineering—Systems, University of Southern California, Los Angeles, CA 90089-2563. Phone: 213-740-4455, FAX: 213-821-1109. M. G. Safonov was supported in part by AFOSR grant F4960-01-1-0302.

successfully deposited the spacecraft into its final orbital slot. The procedure generally consists of a series of slews whose purpose is to scan the payload antenna pattern across receivers pre-positioned on the ground to measure received power. Each slew, in this series of slews, provides a cross-section of the antenna gain pattern (the cross-section often referred to as a "cut"). Stable, high bandwidth attitude control to accomplish the slews, coupled with precise knowledge of spacecraft attitude obtained from Inertial Reference Unit (IRU) measurements (appropriately calibrated before the slews commence) provides all the necessary information to infer the shape of the antenna pattern along with its orientation in a spacecraft fixed coordinate frame (hereafter referred to as the body frame). The appropriate attitude command biases can subsequently be applied to ensure the proper antenna pattern coverage on the ground.

In this paper, unfalsified control theory is applied to the problem of attitude control for antenna mapping. The scope is limited to this challenging attitude control problem. The problems of attitude determination during the slews, related IRU bias calibration, and post-processing of data to provide antenna pattern information are all interesting but beyond the scope of this paper. A simplified simulation model is used to study a model free approach to attitude control. First, in Section 2, a brief outline of unfalsified control theory is provided. Then, in Section 3, the antenna mapping attitude control problem is presented. The set of candidate databank controllers for unfalsified control are described along with the simulation model and relevant dynamics. Finally, in Section 4, simulation results are presented after which a brief conclusion is given.

2. Unfalsified Control Theory

In all engineering disciplines, experimental data provides a most important connection between theory and practice. For control engineers, the situation is no different. Control theory makes no claims about the performance or stability of physical systems, only about their models. The engineer, who is concerned with controlling a physical system, seeks some assurance that closed-loop operation of the actual system can achieve desired performance objectives.

The goals are no different when designing the attitude control laws for a communications satellite. Detailed models of the spacecraft dynamics (derived from complicated finite element models which include thousands of nodes) are employed in the design phase to develop and analyze the control design. Once a control law has been determined, there should be a way of evaluating if available measured data corroborates theoretical predictions of performance. Robust control theory gives powerful techniques for synthesizing control laws, which, theoretically, provide performance and stability guarantees for the closed-loop system. However, as is well known, these techniques require a plant model along with an upper bound on the associated uncertainty (modeling error). Although in spacecraft applications a detailed dynamics model is available, because of uncertainties in material properties, mechanism and joint stiffness, etc. a conservative upper bound is always hypothesized (typically ±25% or more on modal frequencies) which may result in performance limitations (for example, by limiting the controller bandwidth if gain stabilization is required by a customer).

Theory does provide other more rigorous approaches than that suggested above which involve identification of modeling error using experimental data[1,2,3]. These investigations led to the concept of plant model validation[6,7,8] where a model with a hypothesized uncertainty bound is validated against input-output data with the hope that robust controllers based on the model can subsequently be applied if the uncertainty bound proves to be valid (i.e. unfalsified by the data[9]).

So in many control applications, where experimental data from the plant is readily available, the ultimate goal of model validation is to use the validated (unfalsified) plant and uncertainty models along with robust synthesis tools to design control laws which will subsequently be applied to the plant. So that they will only rarely be invalidated, the uncertainty models used are typically conservatively chosen. Thus, even when estimating model error from the data, conservatism may tend to limit the performance attainable with the resultant robust controllers. In addition, choosing the wrong uncertainty structure may also result in undue conservatism.

In satellite applications, a slight wrinkle is added by the fact that experimental data from the plant dynamics are rarely available before launch. And when it is, it may be corrupted by gravity, aerodynamic drag, and other physical phenomena present in the laboratory or test floor, but not in the eventual operational orbit. On the other hand, since satellite retrieval missions are extremely expensive, dangerous and many times even impossible, designers have an imperative to provide control laws with a guarantee of first-pass success.

Unfalsified control provides a way to non-conservatively evaluate the ability of a candidate control law to meet a given performance criterion and the data can be taken with an extremely safe, low-bandwidth controller in place, thus not jeopardizing the health and safety of the spacecraft. In general, it provides a precise, non-conservative approach to evaluating the implications of experimental data regarding the ability of a given control law to meet a given performance criterion, even when the data was collected without that control law in the loop. The concept was first explored in detail by Tsao[4] who worked out the details as it applies to adaptive control formulations. Brozenec[5] subsequently explored many of the theoretical connections of the unfalsified theory with robust control and model validation, demonstrating its non-conservative nature. More recently, falsification techniques were applied to applications ranging from real-time adaptive control of an industrial grinding machine[18] to the retuning of an aircraft autopilot using experimental flight data[17]

The controller validation (unfalsification) problem can be considered for absolutely any control law and any experimentally falsifiable (i.e., testable) performance criterion. Consider the feedback control system of Figure 2. The goal of applying the feedback control law ***K*** to the plant ***P*** is to ensure that the closed-loop system response, call it ***T***, satisfies certain performance criterion. In engineering practice, as already discussed, the plant is always only partially known and, therefore, the system response ***T*** will be uncertain. As a result the ability of the controller ***K*** to ensure a desirable response is also uncertain.

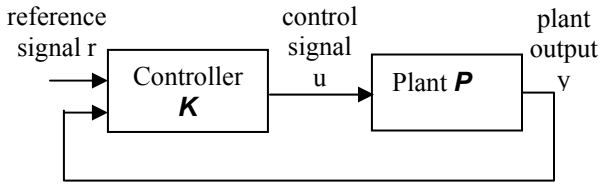

Figure 2. Feedback control system.

For the purpose of discussing controller validation, the input/output description of systems due to Zames[10,11] is helpful. Using this approach, a dynamical system is viewed as a set of input/output pairs (x,y) which are signals in approach functions spaces *X, Y*. In this framework, solutions of feedback interconnections of two systems become the intersection of two graphs in the product space $X\times Y$. For easy visualization, one may view the function spaces as the set of real numbers; for control applications, however, it is often convenient to view the signals as elements of the extend vector space L_{2e}.

Using this viewpoint, we can view the plant and controller as signal constraints (sets) in appropriate function spaces. Consider, again, Figure 2. The plant is a locus or graph in its input/output product space.

(1) $P \subset U \times Y$

where U represents the space of plant input signals and Y the space of plant output signals. Data from a single infinite-time-duration experiment represents a point (u_o, y_o) in the $U \times Y$ -plane on the graph of the plant, which is otherwise unknown. Past data and data from samples of past behavior of is interpolated by (u_o, y_o). In this framework, a control law is regarded as a constraint on the signals *r*, *y*, and *u*. As such, it represents a surface (i.e., a manifold) in the space $R \times Y \times U$

(2) $K \subset R \times Y \times U$.

For example, the controller may compute the control signals u as a linear time-invariant transformation of y and r represented by a transfer function matrix

(3) $$K = \left\{ (r, y, u) \middle| u = K(s) \begin{bmatrix} r \\ y \end{bmatrix} \right\}$$

Likewise, a performance criterion T_{perf} is simply another constraint on the signals r, y, and u and thus represents a subset $T_{perf} \subset R \times Y \times U$ as well.

This characterization of the experimental data, control law, and performance criterion as separate signal constraints provides a convenient framework for presenting the unfalsified control theory[16]. Just as the input-output stability of interconnections of subsystems can be reduced to conditions on intersecting constraints[10,11,12,13,14,15], so the controller validation problem also reduces to conditions on intersecting constraints defined by the data, control law, and performance criterion.

In this context, the controller validation problem can be formulated as follows.

Problem. (Controller Invalidation). Given

1. Measurements of plant input-output signals $(u_o, y_o) \in U \times Y$.
2. A candidate control law $K \subset R \times Y \times U$.
3. A performance criterion $T_{perf} \subset R \times Y \times U$.

Determine whether or not the control law's ability to satisfy the performance criterion is falsified by the data.

The following theorem is a basic result.

Theorem[4,5]. (A Single Experiment). Consider the problem above. ***K*** is unfalsified by the experiment (u_o, y_o) if and only if

(3) $$P_{data} \cap K \subset T_{perf}$$

where

$$P_{data} = \{(r, y, u) \in R \times Y \times U \,|\, y = y_o, u = u_o\}$$

Otherwise, ***K*** is falsified.

The theorem is simple, but communicates clearly what can be determined from the data alone, about the ability of a given control law to meet a given specification. And the statement is a non-conservative if and only if condition which can be applied directly to candidate controllers. Indeed, it suggests a specific process or algorithm for unfalsifying controllers.

Namely, choose a databank set of controllers which are easily parameterized—for example, the well-known and widely used set of Proportional-Integral-Derivative (PID) controllers. For a single-input, single-output PID controller, the control law constraint can be written

(5)

$$K = \left\{ (r, y, u) \,\middle|\, u = \left(C_p + \frac{C_I}{s} + C_d s \right)(r - y) \right\}$$

For this example, the constraint set defined by the experimental data and the controller can be written

(6)

$$P_{data} \cap K = \left\{ (r, y, u) \,\middle|\, r = \hat{k} * u + y, y = y^m, u = u^m \right\}$$

where * denotes convolution and $\hat{k}$ has Laplace transform

(7) $$K(s) = \frac{s}{C_d s^2 + C_p s + C_I}$$

For any candidate controller (parameterized by the three gain values), one only need to check that the set defined by the constraint in (5) falls within the defined performance criterion.

To perform model free adaptive control, one then starts with a candidate controller in the loop; this controller remains in the loop until it is falsified by the data. If so, it is replaced by another candidate controller from the databank which has not yet been falsified. This illustrates the inherent switching nature of the adaptive control when applying unfalsified theory.

3. Antenna Mapping Control Problem

There are two channels in the simplified simulation model for the antenna mapping control problem, the azimuth and elevation channels. The flexible mode is assumed to appear only in the elevation channel with one frequency and zero damping ratio. The quantization and measurement noise are assumed to be present for the position measurements. The PD control law used is

(8) $$u = C_p (r - y) - C_d \dot{y}$$

The performance criterion T_{perf} is chosen to be

(9) $$\begin{cases} |T_{er}(j\omega)| < |W_1^{-1}(j\omega)| \\ |T_{ur}(j\omega)| < |W_2^{-1}(j\omega)| \end{cases}, \forall \omega$$

where $T_{er}(s)$ is the transfer function from r to e=r-y, $T_{ur}(s)$ is the transfer function from r to u, and W_1 and W_2 are weighting transfer functions specifying the error and control responses in frequency domain. In time domain, (9) is equivalent to

(10) $$\begin{cases} \left\| \hat{w}_1 * (r - y) \right\|_{L_2[0,t)} < \left\| r \right\|_{L_2[0,t]} \\ \left\| \hat{w}_2 * u \right\|_{L_2[0,t)} < \left\| r \right\|_{L_2[0,t]} \end{cases}, \forall t, \forall r$$

where $\hat{w}_1$ is the impulse response of W_1 and $\hat{w}_2$ is the impulse response of W_2.

Since (8) is the same as

(11) $r = (1/C_p)u + (C_d/C_p)\dot{y} + y \equiv \theta^T \psi + y$,

where $\theta = [(1/C_p), (C_d/C_p)]^T$ is the controller parameter vector and $\psi = [u, \dot{y}]^T$, given any plant input and output measurements $(u, y, \dot{y})$, and given any controller parameter vector θ, the measurements can be considered as being produced by a "fictitious" reference signal r computed from (11) with the given controller parameter vector in the loop (even though in fact it is not). Hence, any controller parameter vector can be falsified or invalidated if (10) does not hold at any time t for the computed r. On the other hand, if (10) holds for all times up to current time, the controller parameter vector is unfalsified (or not invalidated) by measurements. Based on the information that can be extracted from the available

measurements, all the unfalsified controller parameter vectors should be regarded as equal in their capability to achieve the performance goal.

The following describes how the set of unfalsified controller parameter vectors is defined at any time t, and what the switch method is used in this paper when current controller parameter vector is falsified. Combining equations (10) and (11) gives

$$\begin{cases} \left\|\theta^T\zeta\right\|_{L_2[0,t]} < \left\|\theta^T\psi + y\right\|_{L_2[0,t]} \\ \left\|u\right\|_{L_2[0,t]} < \left\|\theta^T\psi + y\right\|_{L_2[0,t]} \end{cases}, \forall t$$

or

$$(12)\quad \begin{cases} \theta^T A_t^e\theta - 2\theta^T B_t^e + C_t^e < 0 \\ \theta^T A_t^u\theta - 2\theta^T B_t^u + C_t^u < 0 \end{cases}, \text{where}$$

$$A_t^e = \int_0^t \zeta\zeta^T - \psi\psi^T d\tau, B_t^e = -\int_0^t \psi y d\tau, C_t^e = \int_0^t y^2 d\tau$$

$$A_t^u = \int_0^t -\psi\psi^T d\tau, B_t^u = -\int_0^t \psi y d\tau,$$

$$C_t^u = \int_0^t (\hat{w}_2 * u)^2 - y^2 d\tau \text{, and } \zeta = \hat{w}_1 * \psi .$$

At any time t, the set of unfalsified controller parameter vectors is the following intersection $\bigcap_{0<\tau<t} (K_\tau^e(\theta) \cap K_\tau^u(\theta))$ where $K_\tau^x(\theta) = \left\{\theta \middle| \theta^T A_\tau^x\theta - 2\theta^T B_\tau^x + C_\tau^x < 0\right\}$. The solution of set intersection is usually very difficult, especially when A_τ is not positive definite for all τ (i.e., K_τ is not the interior of an ellipsoid at some τ), which is the case here. Fortunately, there are only two parameters in the control law, this makes it easy to find intersections of two quadratic bodies defined by K_τ, thus easy to find an unfalsified vector to switch to when current vector is falsified. For example, let K_τ be the quadratic inequality (12) defined by current measurements. The intersections of K_{st}, a quadratic inequality derived from K_τ with a smaller feasible region obtained by increasing the constant C_t in equation (12), and K_i derived similarly from K_i defined by any previous measurements can be found straightforwardly, see Figure 3. We can find all such intersections for all past measurements, an easy procedure but requires a lot of computation. When the current parameter vector θ is falsified by the current quadratic inequality K_τ, among the intersections found, we choose the one which is not falsified by any past data and is closet to the current θ as the new controller parameter vector to switch to. This is the controller parameter switching method used in our simulation.

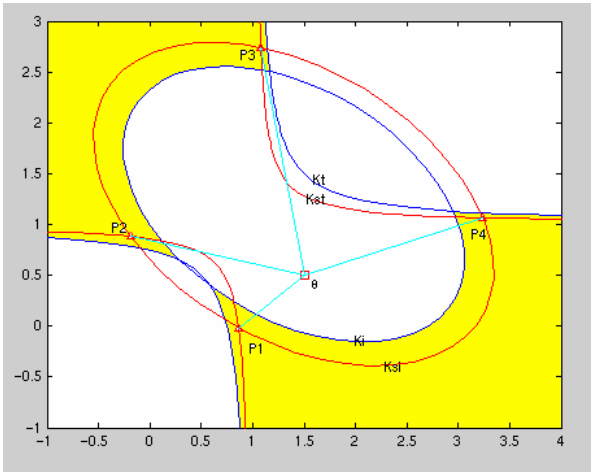

Figure 3. Example of Controller Parameter Switching
The Region of Unfalsified Control Parameter Vectors is in Yellow Color

4. Simulation Results

The following additional constraints on the controller parameter space are used:

1. θ1 is between 5e-6 and 1e4
2. θ2 is between 0 and 1e4
3. $2\theta_1\hat{J} - \theta_2^2 < 0$

where $\hat{J}$ is estimated inertia. The use of constraint 3 above is to ensure the closed loop transfer function has a relatively large damping ratio. The weighting transfer function in Equation (9) is chosen to have its corner frequency of its zeros to be around the solar wing mode.

In our simulation, the weighting transfer function W_1 used for error transfer function is chosen to have a higher bandwidth than the control bandwidth achieved by the nominal non-adaptive controller in order to show the improvement that the unfalsified control method accomplishes. However, because there is a trade off between error response and control energy, the weighting transfer function W_2 used for the control transfer function T_{ur} is chosen such that its inverse has a larger magnitude than that of the closed-loop control transfer function achieved by the nominal non-adaptive controller.

Figure 4 shows the Simulink block diagram used to perform the simulation. The simulation results are shown in Figure 5 to Figure 11.

Figure 5 shows the unfalsified controller parameters stop switching after about 800 seconds. Figure 6 shows the new controller parameters is found by solving the intersection of quadratic equations described in previous section. Figure 7 shows that the magnitude of the achieved transfer function from the reference signal to error signal lies below that of the inverse of the weighting transfer function W_1 used in the unfalsified algorithm. The error transfer function magnitude of the non-adaptive nominal PI controller parameters used for comparison is also shown in the figure. Figure 8 shows that the magnitude of the achieved transfer function from the reference signal to control lies below that of the inverse of the weighting transfer function W_2 used in the unfalsified algorithm.

Figure 9 shows the azimuth channel reference signal. Figure 10 shows that the azimuth pointing error from the unfalsified algorithm is smaller than that produced by the nominal non-adaptive PI controller parameter as expected by the choice of weighting transfer function W_1. Figure 11 is the three wheel control signal. The control signals from the unfalsified control method is larger than those from the nominal non-adaptive controller because the magnitudes of the inverse of the weighting transfer function W_2 used are larger than those of the control transfer function of the latter controller.

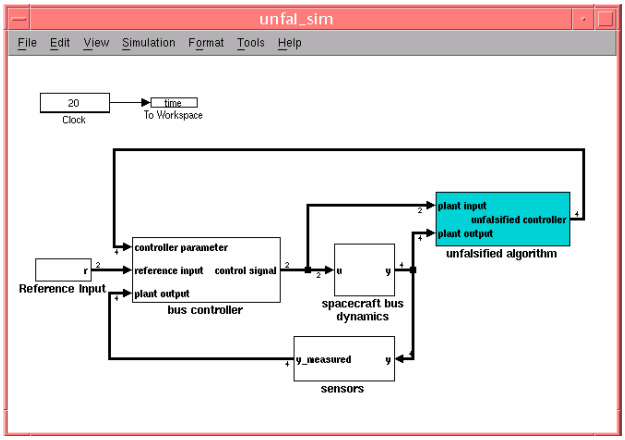

Figure 4. Simulink simulation block diagram.

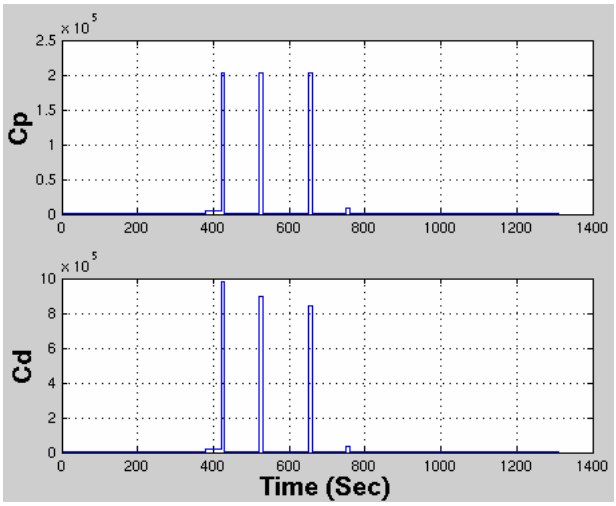

Figure 5. The last switching of unfalsified controller parameters in azimuth channel is at about 800 seconds.

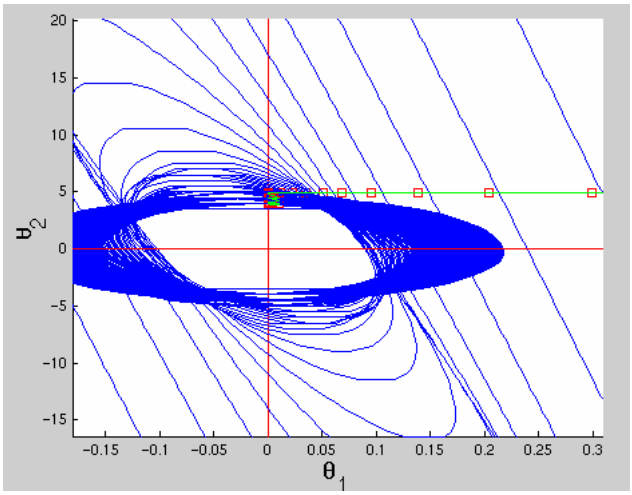

Figure 6. Switching of controller parameter vector.

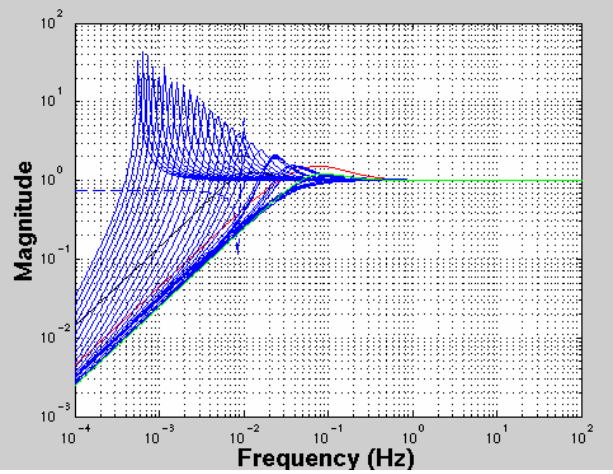

Figure 7. The magnitude of the achieved closed-loop error transfer function Ter (green) lies below that of the inverse of the weighting transfer function W_1(Red). The error transfer function magnitude for nominal non-adaptive parameters used for comparison is shown in black. The initial error transfer function magnitude is shown by the broken blue line.

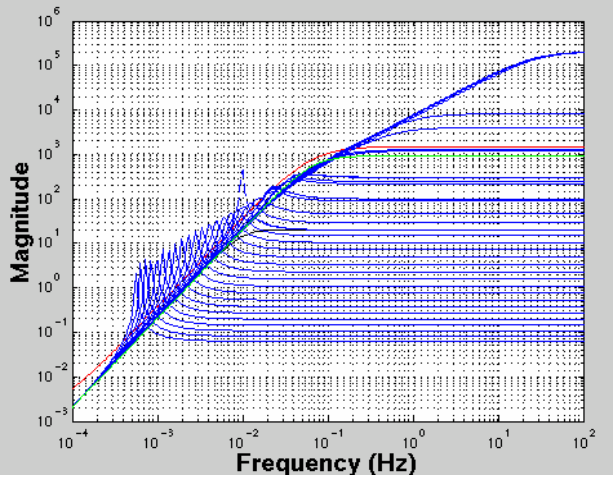

Figure 8. The magnitude of the achieved closed-loop control transfer function Tur (green) lies below that of the inverse of the weighting transfer function W_2 (Red). The control transfer function magnitude for nominal non-adaptive parameters used for comparison is shown in black. The initial error transfer function magnitude is shown by the broken blue line.

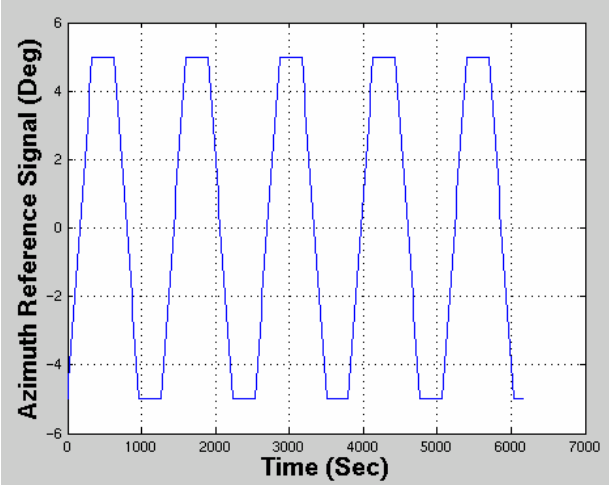

Figure 9. The reference signal in azimuth channel.

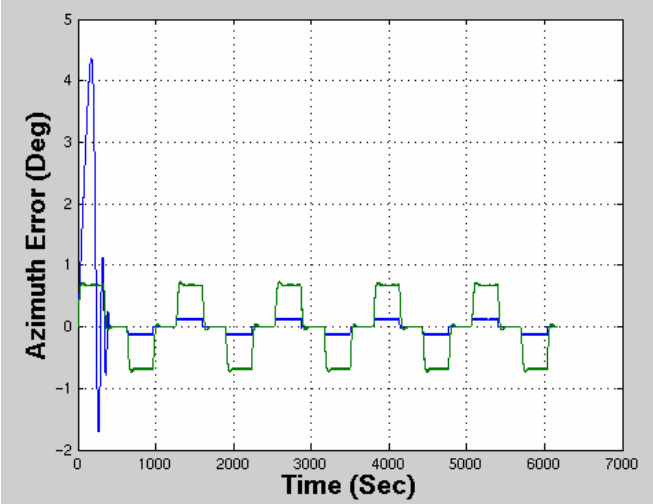

Figure 10. The azimuth error of the unfalsified vontroller (blue) is smaller than that of the nominal non-adaptive controller (green).

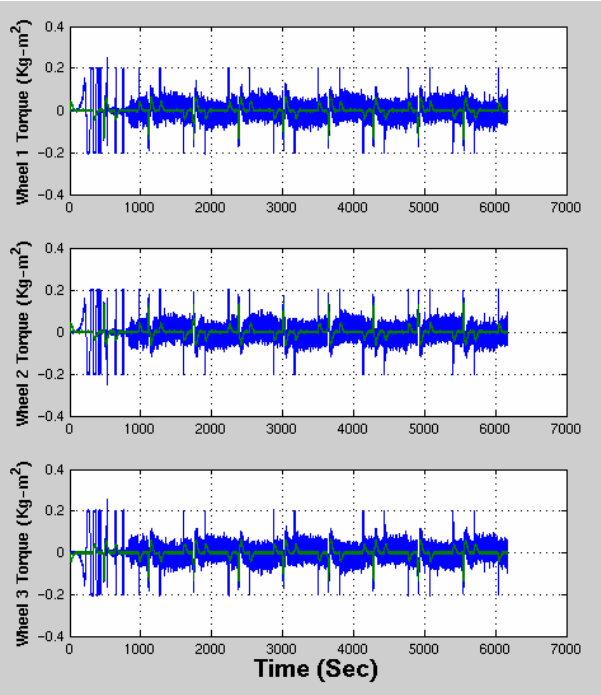

Figure 11. The wheel torques of the unfalsified vontroller (blue) is larger than those of the nominal non-adaptive controller (green).

5. Conclusions

This paper demonstrates that, with only approximate knowledge of the spacecraft inertia and mode location, the proposed unfalsified adaptive control method is able to find PI controller parameters that achieve a given performance specification.

References

1. R.L. Kosut. Adaptive Calibration: An Approach to Uncertainty Modeling and On-Line Robust Control Design. In: *Proceedings of the IEEE Conference on Decision and Control*. pp. 455-461, 1986
2. R.L. Kosut, M.K. Lau, and S.P. Boyd. Set Membership Identification of Systems with Parametric and Nonparametric Uncertainty. *IEEE Transactions On Automatic Control* **37**(7), 929-941, 1992.
3. A. Helmicki, C. Jacobson, and C. Nett. Control Oriented System Identification: A Worst-Case Deterministic Approach in H_∞. *IEEE Transactions on Automatic Control* **36**(5), 1163-1176, 1991.
4. Tung-Ching Tsao. Set Theoretic Adaptor Systems. PhD Thesis. 1993. University of Southern California. Los Angeles, CA.
5. T.F. Brozenec. Controller Validation, Identification and Learning. PhD Thesis, 1996. University of Southern California. Los Angeles, CA.
6. R. Smith and J. Doyle. Model Validation – A Connection Between Robust Control and Identification. *IEEE Transactions on Automatic Control* **37**(7), 942-952, 1992.
7. R. Smith and J. Doyle. Model Validation and Parameter Identification for Systems in H_∞ and l_1. In: *Proceedings of the American Control Conference*, pp. 2852-2856, 1992.
8. K. Poolla, P. Khargonnekar, A. Tikku, J. Krause, and K. Nagpal. A Time-Domain Approach to Model Validation. *IEEE Transactions on Automatic Control* **39**(5), 952-959, 1994.
9. J.C. Willems. Paradigms and Puzzles in the Theory of Dynamical Systems. *IEEE Transactions on Automatic Control*, AC-36: 259-294, 1991.
10. G. Zames. On the Input-Output Stability of Time-Varying Systems – Part I: Conditions Derived Using Concepts of Loop Gain, Conicity, and Positivity. *IEEE Transactions On Automatic Control* **15**(2), 228-238, 1966.
11. G. Zames. On the Input-Output Stability of Time-Varying Systems – Part II: Conditions Involving Circles in the Frequency Plane and Sector Nonlinearities. *IEEE Transactions On Automatic Control* **15**(3), 465-467, 1966.
12. G. Zames. Functional Analysis Applied to Nonlinear Feedback Systems. *IEEE Transactions on Circuit Theory* **CT-10**, 392-404, 1963.
13. I.W. Sandburg. A Frequency Domain Condition for the Stability of Feedback Systems Containing a Single Time-Varying Element. *Bell system Technical Journal* **43**(4), 1601-1608, 1964.
14. I.W. Sandburg. On the L2-boundedness of Solutions of Nonlinear Functional Equations. *Bell System Technical Journal* **43**(4), 1581-1599, 1964.
15. M.G. Safonov. *Stability and Robustness of Multivariable Feedback Systems*. MIT Press. Cambridge, MA, 1980.
16. M.G. Safonov and T. Tsao. The Unfalsified Control Concept and Learning. *IEEE Transactions On Automatic Control* **42**(6), 843-847, 1997
17. F. Demourant, G. Ferreres, and Jean-Marc Biannic. Falsification of an Aircraft Autopilot.

Proceedings of the American Control Conference, Anchorage, AK, pp. 803-808, 2002.

18. H. A. Razavi and T. R. Kurfess. Force control of a reciprocating surface grinder using unfalsification and learning concept. *Int J Adaptive Control and Signal Processing*, **15**(5):503—518, August 2001.